

Generation of coherent phonons in bismuth by ultrashort laser pulses in the visible and NIR: displacive versus impulsive excitation mechanism.

A.A. Melnikov^{1,2}, O.V. Misochko³, and S.V. Chekalin¹

¹*Institute of Spectroscopy, Russian Academy of Sciences, 142190 Troitsk, Moscow region, Russia*

²*Moscow Institute of Physics and Technology, 141700 Dolgoprudny, Moscow region, Russia*

³*Institute of Solid State Physics, Russian Academy of Sciences, 142432 Chernogolovka, Moscow region, Russia*

We have applied femtosecond pump-probe technique with variable pump wavelength to study coherent lattice dynamics in Bi single crystal. Comparison of the coherent amplitude as a function of pump photon energy for two different in symmetry E_g and A_{1g} phonon modes with respective spontaneous resonance Raman profiles reveals that their generation mechanisms are quite distinct. We show that displacive excitation, which is the main mechanism for the generation of coherent A_{1g} phonons, cannot be reduced to the Raman scattering responsible for the generation of lower symmetry coherent lattice modes.

PACS numbers: 78.47.-p, 78.47.J-

When ultrashort laser pulses interact with solids they can excite lattice vibrations showing high degree of temporal and spatial coherence [1-3]. These coherent phonons reveal themselves as damped oscillations of a certain optical parameter (e.g. reflectivity or transmittance) in the time domain. One of the most important and still unclear aspects of this phenomenon is the mechanism by which the collective atomic motion is generated. To create coherence one needs to establish fixed phase relations either among different q modes of the same phonon branch [4], or between vacuum and excited states of a single $q \approx 0$ phonon mode [5]. Coupling of these lattice states can be achieved in two distinct ways. First, owing to the large spectral bandwidth of an ultrashort laser pulse, it can generate nonstationary phonon states in a crystal through impulsive stimulated Raman scattering, providing a kick to the atoms of the crystal [6, 7]. In this case, which we will further refer to as Raman mechanism (RM), the coherence is “field driven”, with the driving force responsible for both the energy and coherence transfer from electromagnetic field to lattice. Apart from the “field

driven” coherence directly prepared by laser radiation, lattice coherence can also be driven by rapid nonradiative processes. For opaque crystals that have long-lived excited states, the excited state coherence is usually dominant [1-3]. To describe the creation of coherence in this case the displacive excitation of coherent phonons (DECP) model was introduced [8]. In contrast to RM, for DECP the lattice coherence is “relaxation driven” with no momentum imparted to the atoms from the pump pulse.

In an attempt to describe the creation of lattice coherence within a unified approach it was suggested that DECP is not a distinct mechanism, but a particular (resonant) case of RM [9, 10]. Further elaboration of this Raman-based model included the effects of finite lifetime of the intermediate state on the phase and amplitude of coherent phonons [11]. One way to figure out which of the models provides a physically correct description is to measure the initial phase of observed oscillations, as the initial phase, to the first approximation, reveals the excitation mechanism: sine-like for RM and cosine-like for DECP. However, in the present study an alternative approach is used. To clarify the generation mechanism, we have measured the dependence of coherent phonon amplitude of fully symmetric A_{1g} and doubly degenerate E_g phonon modes in bismuth on excitation wavelength in visible and near infrared ranges. According to the unified Raman model, the coherent phonon amplitudes should be proportional to the corresponding Raman cross sections. Moreover, at any given wavelength the relative intensities of excited phonon modes obtained from the frequency- and time-domain data should be identical. Yet, a comparison of our pump-probe results with spontaneous Raman measurements obviously contradicts the predictions of the unified Raman theory.

In our experiments all measurements were done at room temperature with a typical ultrafast pump-probe setup. Amplified pulses of a Ti:Sapphire laser operating at $\lambda=800$ nm were divided into two parts. The first was attenuated to be used to probe the sample – a single crystal of bismuth oriented in such a way that its surface was perpendicular to the trigonal axis. The second part of the beam was used to seed a parametric amplifier to provide pump pulses of 70 fs duration with a tunable central wavelength. The pump and probe beams were incident nearly perpendicular to the surface of the crystal. We detected a component of the probe beam reflected from the crystal and polarized parallel to the pump polarization, while the incident probe pulses were polarized at 45° relative to the pump. Energy of this component was measured with opened and closed pump beam and the relative change in reflectivity $\Delta R/R_0$ was recorded at a given time delay between the pump and probe pulses.

Figure 1 shows the transient reflectivity obtained with pump wavelengths of $\lambda=400$ and $\lambda=1300$ nm. Ultrafast excitation at $t=0$ is followed by a monotonic decay on which pronounced oscillations are superimposed. Since the dominant oscillation frequency almost matches that of A_{1g} phonon mode, these oscillations are the result of fully symmetric A_{1g} coherent atomic motion induced by the laser pulse. It should be noted that the detected A_{1g} vibrations demonstrate approximately cosine-like behavior in accordance with previous experimental results [8]. At positive time delays the transient reflectivity excited by the $\lambda=400$ nm pump pulses can be well fitted by the sum of a damped cosine and a monotonic term:

$$\Delta R/R_0 = A(A_{1g}) \exp(-\gamma_1 t) \cos(\nu_1 t) + B(t) \quad (1)$$

where $A(A_{1g})$ is the amplitude and γ_1 - is the decay rate of coherent oscillations with the frequency $\nu_1 = 2.93$ THz. The exact form of $B(t)$ term is of no importance in the present study; however, we note that the term has a multi-exponential character.

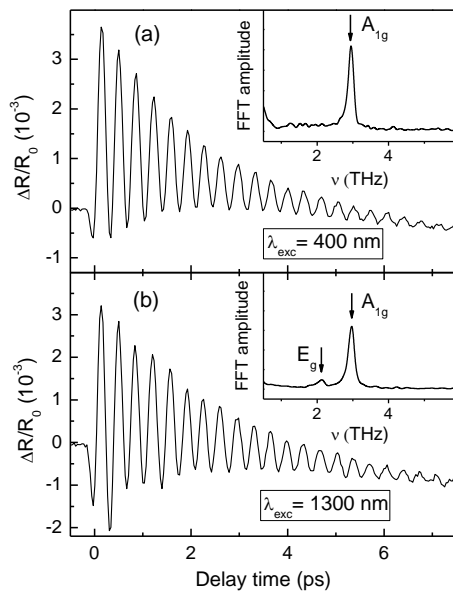


Fig. 1. (a) Transient reflectivity of bismuth excited at $\lambda=400$ nm as a function of time delay. The inset shows normalized Fourier spectrum for the oscillatory part of the signal. (b) The same curves for the case of $\lambda=1300$ nm excitation. Note that in the inset apart from the A_{1g} mode, the E_g mode is clearly visible.

The photoinduced response described by Eq. (1) is typical for bismuth and it has been

observed in numerous previous experiments (see e.g. [8, 12, 13]). Fully symmetric A_{1g} coherent contribution always dominates in the transient reflectivity obtained by isotropic detection at room temperature, while doubly degenerate E_g oscillations are almost negligible. The latter appear either at low temperatures [14], or at high excitation densities (alternatively, they can be observed at room temperature by a special detection technique such as electrooptic sampling [15]). In contrast, our results clearly demonstrate that it is possible to select a particular excitation wavelength at which the amplitude of E_g oscillations is relatively large (reaching up to one fourth of A_{1g} coherent amplitude). And this can be achieved at room temperature by means of isotropic detection. Indeed, as follows from Fig. 1(b), during the first few picoseconds the transient reflectivity excited by long wavelength 1300 nm pump pulses shows a considerable deviation from that excited by the short wavelength pulses. Its Fourier spectrum shown in the inset indicates that the main difference is due to the presence of strongly damped oscillations at ~ 2.1 THz, which can be naturally ascribed to the coherent phonons of E_g symmetry [13]. With a good accuracy these oscillations demonstrate sine-like behavior, and thus, the overall time-resolved signal can be represented in the following form:

$$\Delta R/R_0 = A(A_{1g})\exp(-\gamma_1 t)\cos(\nu_1 t) + A(E_g)\exp(-\gamma_2 t)\sin(\nu_2 t) + B(t) \quad (2)$$

where $A(E_g)$, γ_2 , ν_2 are the amplitude, the decay rate and the frequency of E_g oscillations. To obtain the amplitudes $A(A_{1g})$ and $A(E_g)$ we fitted the experimental data by Eq. (2). It should be noted that due to significant difference in the parameters of A_{1g} and E_g oscillations this fitting procedure is quite unambiguous and thus allows achieving a satisfactory precision. As a result of the fitting, for the 1300 nm excitation we obtained the following oscillatory parameters: $A(A_{1g}) = (1.2 \pm 0.1) \cdot 10^{-3}$ and $A(E_g) = (3 \pm 0.5) \cdot 10^{-4}$ for coherent amplitudes (the amplitude ratio of ~ 4) and $\gamma_1 = 0.5 \text{ ps}^{-1}$ and $\gamma_2 = 1.5 \text{ ps}^{-1}$ for the decay rates.

To measure varying amplitudes of the coherent oscillations excited in the near infrared and visible, a set of excitation wavelengths ranging from 400 to 2500 nm was used. In each case, the pump spot size and bismuth reflectivity were taken into account to ensure equal intensity of the pump field for all the wavelengths used (if measured inside the sample, near the surface). It was found that when the latter condition to be fulfilled, the monotonic part of the signal $B(t)$ together with decay rates of the oscillations were almost independent of excitation wavelength. At the same time, the amplitudes of coherent phonons demonstrated significant spectral variation, essentially different for A_{1g} and E_g modes. Figure 2(a) illustrates the observed wavelength dependence of amplitude for fully symmetric and doubly degenerate modes. One can see that the amplitude of E_g oscillations is close to zero in the

visible range for the wavelengths of $\lambda=400, 600$ and 700 nm. However, starting from $\lambda \geq 800$ nm the E_g amplitude begins to grow reaching its maximum near $\lambda=1300$ nm (~ 1 eV). In contrast, the amplitude of A_{1g} phonons remains approximately constant in the visible and near infrared range up to $\lambda=1300$ nm. For excitation wavelengths larger than $\lambda=1800$ nm (~ 0.7 eV), the generation efficiency for both phonon modes exhibits a sharp decrease.

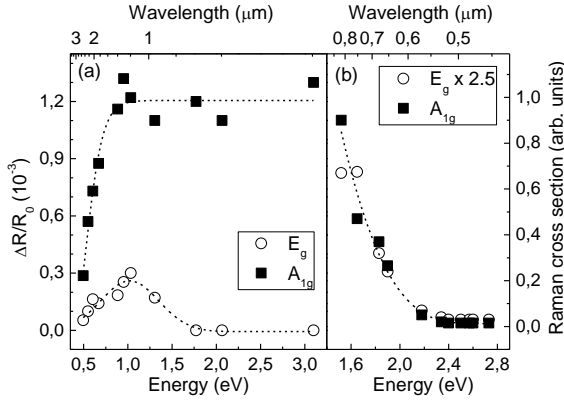


Fig. 2. (a) Amplitudes of E_g and A_{1g} coherent oscillations as a function of excitation photon energy. (b) Resonance profile of the Raman cross sections of E_g and A_{1g} phonon modes of bismuth measured in [16]. Dashed lines are a guide to the eye.

In order to clarify the generation mechanism, we compared the amplitudes of A_{1g} and E_g modes obtained in our time-resolved experiments with the corresponding Raman cross sections measured in the 1.55-2.7 eV range [16] and reproduced in Fig. 2(b). We found that only for E_g mode the Raman cross section and the coherent phonon amplitude demonstrate similar behavior on excitation wavelength (here we have disregarded a longer tail in the short wavelength range). A limited excitation range used in the cited Raman study doesn't allow to find out the exact maximum position of this resonance profile, however, there was suggested that the most effective Raman scattering should take place for photon energies in the vicinity of E_1 critical point of bismuth (1.2 eV) [16]. This similarity of time- and frequency domain resonance results speaks in favor of a Raman-like excitation mechanism for the coherent phonons of E_g symmetry. The set of data points shown in Fig. 2(a) for E_g phonons can be approximated by a bell-like shape, which implies that the process of coherent E_g phonon generation is a resonant one at long wavelength excitation. This, in combination with a sine-like temporal behavior of oscillations, allows attributing the generation mechanism for E_g

phonons to resonant Raman scattering. The maximum of E_g amplitude located around ~ 1 eV then corresponds to a real transition between certain electronic energy levels (unlike virtual transitions typical for off-resonance Raman scattering in a transparent crystal). When the carrier frequency of a pump femtosecond pulse approaches this energy, the Raman cross-section increases strongly. If the central wavelength is detuned from resonance, the generation efficiency of coherent phonons drops, making the detection of E_g component by standard pump-probe technique barely possible.

In contrast to E_g oscillations, the dependence of fully symmetric A_{1g} coherent amplitude on pump wavelength is essentially different from the resonance profile of A_{1g} scattering cross section. Indeed, the A_{1g} phonons are generated effectively only when the energy of pump photons exceed a critical value that can be roughly defined as ~ 0.7 eV. If this condition is fulfilled, the amplitude, and even the whole photoinduced response (if we ignore E_g oscillations and a small additive constant), demonstrate almost no dependence on excitation wavelength. This result is essentially different from that obtained in [10] with degenerate pump-probe technique for fully symmetric phonons in Sb and used to support the unified Raman model. The observed discrepancy between the A_{1g} resonance Raman profile and the pump wavelength dependence allows suggesting that RM in the case of fully symmetric phonons of bismuth is not effective. Indeed, if both A_{1g} and E_g modes were excited by the same Raman-like mechanism, the amplitude of higher frequency A_{1g} mode would be reduced in comparison to the amplitude of low frequency E_g mode (thus their amplitude ratio would be smaller than in the frequency domain). This is a direct consequence of different ratios between the pulse bandwidth and the phonon frequency that define the efficiency of coherent phonon generation: the larger the ratio, the more effective is the generation. However, in the experiment we observe the opposite situation: the amplitude ratio in the time domain is significantly larger than in the frequency domain. To demonstrate the dependence of coherent amplitude on the bandwidth/frequency ratio, we measured it for fully symmetric phonons by changing the pump pulse duration. The result shown in Fig. 3 indicates that the corresponding dependence is almost exponential. It can be characterized by the factor $e^{-t/\tau}$, where t is the pump pulse duration and τ is equal to approximately one quarter of inverse phonon frequency. Thus, in the time-domain the amplitude ratio for A_{1g} and E_g modes should be around 1.5, instead of more than 10 observed at excitation wavelengths away from resonance at $\lambda=1300$ nm.

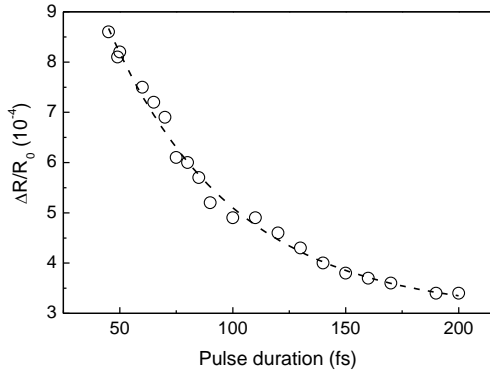


Fig. 3. Coherent A_{1g} amplitude as a function of pulse duration. The dashed line is an exponential fit. The data were obtained in a degenerate pump-probe scheme at $\lambda=800$ nm. The probe pulse was always transform limited one with duration of 45 fs.

In an attempt to explain the specific shape of the wavelength dependence for A_{1g} phonon amplitude we have analyzed linear optical properties of bismuth and found out that $A(A_{1g})$ correlates not with the resonance Raman profile but with the absorption spectrum of the crystal. To illustrate this we show in Fig. 4 the absorption coefficient k and the penetration depth d calculated from ellipsometric data [17]. It can be seen that the absorption coefficient k exhibits a sharp decrease when the photon energy changes from 1 to 0.25 eV, just like the fully symmetric coherent amplitude. Such a similarity suggests that the lattice state just after ultrafast excitation is primarily controlled by the amount of absorbed energy.

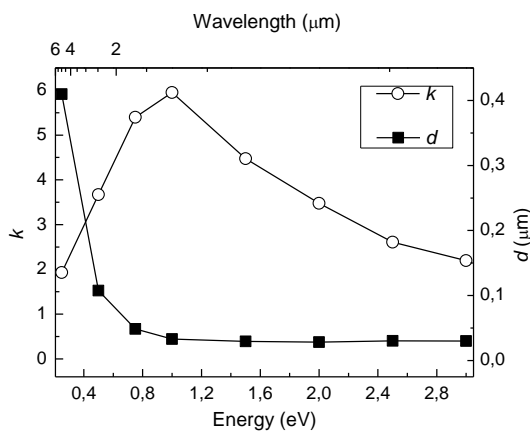


Fig. 4. Absorption coefficient k and penetration depth d of bismuth as a function of photon energy calculated using the data provided in [17].

The only necessary correction is caused by the fact that the probe wavelength in all our measurements is fixed and therefore, the same volume is probed for every excitation wavelength. When the pump wavelength differs from $\lambda=800$ nm, which is our probe wavelength, the absorption length varies and so does the excited volume. Thus, to treat the effect of absorption on coherent phonon amplitude properly, one should compare $A(A_{1g})$ with penetration depth d . Indeed, as follows from the comparison of data presented in Fig. 2(a) and Fig. 4, corresponding dependences are almost identical.

The key role of the amount of absorbed energy and extraordinary high efficiency for fully symmetric coherent phonons naturally suggest that the generation mechanism in this case should be considered as purely displacive one. Indeed, rhombohedral bismuth has a Peierls-distorted lattice, which is highly sensitive to the state of electronic subsystem. Specifically, the increased number of excited electrons near the Fermi level can significantly alter interatomic potential. At the same time, the discussed A_{1g} mode is remarkable as only its symmetry coincides with that of the Peierls shift [8]. Thus, the fully symmetric atomic oscillations can be launched by an ultrashort laser pulse if and only if a considerable part of pump pulse energy has been absorbed, creating a nonequilibrium electronic distribution. This process is completely different from the Raman excitation of coherent phonons. If in the Raman mechanism an ultrashort light pulse literally kicks the lattice, sending it into motion, and the momentum and energy transferred in this kick depend on the strength of the light pulse alone, in DECP the laser pulse kicks the potential and the energy conveyed to the lattice basically depends on excited charge density. RM is a *direct* two-photon process, while DECP is a *two-step* process, which essentially depends on the relaxation of excited electron density. Their counterparts in the frequency domain are resonant Raman scattering and hot luminescence, respectively [18]. The major difference between the two time-domain processes is that RM relies on the transverse relaxation creating lattice coherence due to laser field coherence, whereas DECP is affected by the longitudinal relaxation and produces lattice coherence by a rapid nonradiative process. Our results show that in the case of A_{1g} oscillations in bismuth this nonradiative process is electronic thermalization. Indeed, laser pulses with photon energy in the visible range produce nearly identical photoinduced responses and, in particular, fully symmetric coherent phonons of equal amplitude. Therefore, the coherent excited state is formed through the redistribution of energy of highly nonequilibrium charge carriers. Since thermalization is faster than inverse period of A_{1g} oscillations, the generation of coherent atomic vibrations becomes possible.

In summary, we have measured the amplitude of coherent phonons of A_{1g} and E_g symmetry in bismuth in visible and near infrared ranges and found some evidences against the unified Raman model. The comparison of the obtained data to spontaneous Raman cross sections and absorption spectrum allowed us to directly differentiate between DECP mechanism for A_{1g} and Raman mechanism for E_g phonon modes. While fully symmetric lattice dynamics is governed by the excited electronic density, the doubly degenerate phonon mode is “field driven” and demonstrates a distinct resonance behavior. The latter circumstance makes it possible to generate E_g coherent phonons with 1:4 ratio for E_g to A_{1g} amplitudes by using the pump wavelength of $\lambda=1300$ nm. Based on the observed differences for E_g to A_{1g} coherent modes, we conclude that displacive excitation, which requires a fast longitudinal relaxation, cannot be reduced in the case of Bi to Raman scattering based on transverse relaxation.

References

1. L. Dhar, J. A. Rogers, and K. A. Nelson, *Chem. Rev.* **94**, 157 (1994).
2. R. Merlin, *Solid State Commun.* **102**, 207 (1997).
3. O.V. Misochko, *JETP* **92**, 246 (2010).
4. R. Scholz, T. Pfeifer, and H. Kurz, *Phys. Rev. B* **47**, 16229 (1993).
5. A. V. Kuznetsov and C. J. Stanton, *Phys. Rev. Lett.* **73**, 3243 (1994).
6. Y. Yan and K. A. Nelson, *J. Chem. Phys.* **87**, 6240 (1987).
7. A. M. Walsh and R. F. Loring, *Chem. Phys. Lett.* **160**, 299 (1989).
8. H. J. Zeiger *et al.*, *Phys. Rev. B* **45**, 768 (1992).
9. G. A. Garrett *et al.*, *Phys. Rev. Lett.* **77**, 3661 (1996).
10. T. E. Stevens, J. Kuhl, and R. Merlin, *Phys. Rev. B* **65**, 144304 (2002).
11. D. M. Riffe and A. J. Sabbah, *Phys. Rev. B* **76**, 085207 (2007).
12. M. Hase *et al.*, *Phys. Rev. B* **55**, 5448 (1998).
13. M. Hase *et al.*, *Phys. Rev. Lett.* **88**, 067401 (2002).
14. K. Ishioka, M. Kitajima, and O.V. Misochko, *J. Appl. Phys.* **100**, 093501 (2006).
15. M. Hase *et al.*, *Appl. Phys. Lett.* **69**, 2474 (1996).
16. J. B. Renucci *et al.*, *Phys. Status Solidi (b)* **60**, 299 (1973).
17. P. Y. Wang and A. L. Jain, *Phys. Rev.* **2**, 2978 (1970).
18. Y. R. Shen, *Phys. Rev. B* **9**, 622 (1974).